Electron-Transfer Reactions in Micelles: Dynamics of Psoralen and Coumarin Radical Cations

L. Chen, P. D. Wood, A. Mnyusiwalla, J. Marlinga, and L. J. Johnston*

Steacie Institute for Molecular Sciences, National Research Council Canada, Ottawa, Ontario K1A 0R6, Canada

Received: July 17, 2001; In Final Form: August 27, 2001

Radical cations of several psoralens and coumarins have been generated by photoionization in aqueous micellar solution for a comparison of their dynamic behavior with results observed previously in aqueous solution. The photoionization efficiencies are significantly higher in anionic sodium dodecyl sulfate (SDS) micelles than in aqueous solution as a result of favorable electrostatic effects that lead to rapid ejection of the electron into the aqueous phase. By contrast, much lower quantum yields are measured in neutral and cationic micelles. Experiments with anionic quenchers that are soluble only in the aqueous phase demonstrate that exit of the radical cations from anionic SDS micelles is too slow to measure ($<10^5$ s^{-1}) under our conditions. Exit rate constants from neutral Triton X-100 micelles are approximately an order of magnitude faster. Comparison of equilibrium constants for both triplet and radical cations of 4,5′,8-trimethylpsoralen demonstrates that electrostatic effects lead to an order of magnitude enhancement of the affinity of the radical cation for the anionic vs neutral micelles, as compared to the triplet of the same substrate. The slow exit of the radical cation from the micelle facilitates the measurement of rate constants for reaction of the micelle-incorporated radical cations with both water soluble quenchers and species for which exchange between micelle and aqueous phases is rapid on the time scale of the radical cation lifetime. This work provides some of the first kinetic data for dynamics of exit of reactive radical cations from micelles and indicates that these species may provide useful probes for studying electron-transfer dynamics in micellar media.

Introduction

Micelles have been extensively used as models for understanding the effects of heterogeneous environments on reaction dynamics and mechanisms.[1−7] They provide a simple model for understanding electron-transfer processes that are important in energy storage and conversion and for understanding the complex behavior encountered in biological assemblies. We have recently studied the photoinduced electron-transfer chemistry of psoralens and coumarins in aqueous solution[8−10] and have now extended this work to studies in micellar solution to elucidate the role of the environment on psoralen photochemistry.

Previous results show that a variety of psoralens and coumarins undergo reasonably efficient photoionization upon 355 nm excitation in aqueous solution.[8−10] The resulting radical cations react with easily oxidizable substrates such as amino acids and nucleotides, primarily via electron-transfer reactions. This raises the possibility that electron-transfer chemistry may play a role in the clinical use of these compounds. The combination of psoralens and UVA irradiation (PUVA therapy) has been used for the last 2 decades for the treatment of dermatological disorders.[11−13] More recently, psoralens have been investigated for other applications such as treatment of T-cell lymphoma and purification of blood products.[14] The phototherapeutic effects of psoralens are believed to result from intercalation of the drug between adjacent base pairs in the DNA duplex, followed by two successive photocycloaddition reactions that cross-link the DNA. This leads to inhibition of replication and hence cell proliferation. Despite the widespread use of PUVA therapy, there is increasing evidence that its long term use may have deleterious side effects.[15−17] As a result, considerable attention has been focused on understanding the involvement of non-DNA-specific processes in psoralen photochemistry. In addition to the electron-transfer chemistry noted above, singlet oxygen, photocycloadditions to membrane components, and protein binding have all been shown to be important.[18−22] Thus, it is clear that understanding both the therapeutic and harmful effects of psoralens will require a detailed understanding of the effects of the local microenvironment on controlling the competition between reaction pathways.

As an initial step toward understanding the role of the local environment on psoralen reactivity, we have studied the effects of organized media such as micelles, vesicles, and protein complexes on psoralen and coumarin photochemistry. Herein, we report our results in micellar solution, in which we have focused on determining the efficiency with which photoionization occurs in micellar media and the fate of the product radical cations. Significantly enhanced photoionization yields are measured in anionic sodium dodecyl sulfate (SDS) micelles relative to aqueous solution for several psoralens and coumarins (Chart 1); by contrast, decreased yields are observed in both cationic and neutral micelles. These results are attributed to electrostatic effects on the efficiency of cage escape of the initial geminate ion pair. Detailed kinetic studies in the presence of anionic quenchers indicate that exit of radical cations from the micelle occurs with rate constants of less than 10^5 s^{-1} for SDS and is at least an order of magnitude faster for Triton X-100. The slow exit of the radical cations from SDS micelles allows

10.1021/jp0127420 CCC: $20.00 Published 2001 by the American Chemical Society
Published on Web 10/04/2001

CHART 1

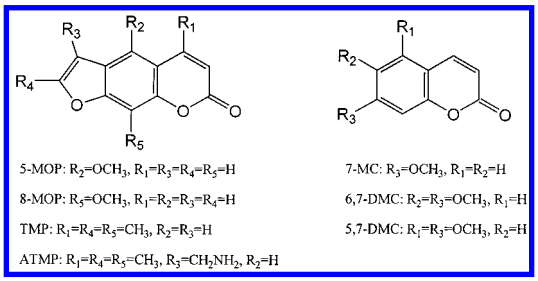

one to measure quenching rate constants without resorting to complex kinetic models for quenchers that are soluble only in the aqueous phase or that exchange rapidly between the two phases. Data for electron-transfer reactions with several biological substrates are measured and compared to those in aqueous solution. The results demonstrate the importance of the environment in controlling the competition between various reaction pathways. In addition, radical cations may provide useful probes for assessing the effects of micelles on electron-transfer rates because they can be used over a wider range of time scales than the fluorescent singlet states that are frequently used for such purposes.[23]

Experimental Section

Materials. 7-Methoxycoumarin (7-MC), 5,7-dimethoxycoumarin (5,7-DMC), 6,7-dimethoxycoumarin (6,7-DMC), 5-methoxypsoralen (5-MOP), 8-methoxypsoralen (8-MOP), 4,5′,8-trimethylpsoralen (TMP), *trans*-8,*trans*-10-dodecadien-1-ol, 2,5-dimethyl-2,4-hexadiene, Triton X-100, and sodium nitrite were purchased from Aldrich and used without further purification. 4′-Amino-4,5′,8-trimethylpsoralen (ATMP), guanosine, guanosine 5′-monophosphate (GMP), tryptophan, and L-histidine were commercial samples from Sigma and used as received. Sodium dodecyl sulfate (SDS, Sigma) and cetyltrimethylammonium bromide (CTAB, Aldrich) were recrystallized from ethanol and methanol, respectively. All solvents were of the highest available commercial grade (Omnisolv).

Laser Flash Photolysis. The nanosecond laser flash photolysis system has been described in detail elsewhere.[24] The excitation source was either a Lumonics HY750 Nd:YAG laser (355 nm, 40 mJ/pulse, 10 ns/pulse) or a Lumonics EX530 excimer laser (XeCl, 308 nm, 40 mJ/pulse, 6 ns/pulse). All solutions were prepared in either potassium phosphate buffer (pH = 7) or aqueous micelle solution. Samples were contained in a 7 × 7 mm^2 quartz cell and prepared at concentrations (typically (1−2) × 10^{-4} M) needed to give absorbances in the range of 0.4−0.5 at the excitation wavelength unless otherwise stated. Ground-state UV−visible absorption spectra were recorded on a Varian CARY 3 spectrophotometer. Samples were purged with nitrogen or oxygen for a minimum of 2 min/mL prior to laser irradiation.

Quantum Yields of Photoionization. Photoionization quantum yields for psoralens or coumarins were determined by comparative actinometry using benzophenone in N_2-purged benzene as the actinometer ($\Phi_T = 1$; $\epsilon_T = 7870$ M^{-1} cm^{-1} at 525 nm).[25] The laser energy dependence of the yield of benzophenone triplet at 525 nm was compared to that of the solvated electron at 700 nm for an optically matched solution of psoralen or coumarin. The decay profiles were extrapolated back to zero time to obtain the initial signal intensities. The slopes of the two laser energy dependence plots were substituted in eq 1, along with a value of 18 000 M^{-1} cm^{-1} for $\epsilon_{e^-(s)}$[26], to give the quantum yield for formation of the solvated electron, $\Phi_{e^-(s)}$, and hence the photoionization quantum yield for the psoralen or coumarin, Φ_{pi}.

$$\Phi_{pi} = \Phi_{e^-(s)} = \frac{\text{slope}_{e^-(s)}\epsilon_T^{BZP}}{\text{slope}_{BZP}\epsilon_{e^-(s)}}\Phi_T^{BZP} \quad (1)$$

Fluorescence Spectroscopy. Fluorescence emission spectra were recorded with a Photon Technology International fluorescence spectrometer. Samples were contained in a 10 × 10 mm^2 quartz cuvette and prepared immediately prior to use with absorbances of less than 0.1 at an excitation wavelength corresponding to the absorption maximum for the specific psoralen or coumarin.

The change in fluorescence intensity as a function of added surfactant was used to estimate an approximate equilibrium constant for partitioning of 6,7-DMC and TMP between aqueous and micellar phases (eq 2; S = substrate, M = micelle). A

$$S + M \overset{K}{\rightleftharpoons} S{-}M \quad (2)$$

double reciprocal plot according to eq 3, (where I_0, I_{inf}, and I_t

$$\frac{I_{inf} - I_0}{I_t - I_0} = 1 + \frac{1}{K[M]} \quad (3)$$

are the fluorescence intensities in water, at 100% incorporation in micelles, and in intermediate micelle concentrations) gives an estimate of K from the intercept and slope of plots of $1/(I_t - I_0)$ vs $1/[M]$ for cases where the fluorescence lifetime of the probe differs in water and in micelles.[27,28] The measurements of fluorescence intensity were carried out at constant substrate concentration, and the change in the UV−vis spectrum of the substrate as a function of added surfactant was negligible. Intensities were measured at the fluorescence maximum. Analysis of the data according to eq 3 gave estimates of partition coefficients of ∼8000 M^{-1} for 6,7-DMC and TMP in SDS and for 6,7-DMC in Triton X-100; a slightly higher value of 12 000 M^{-1} was estimated for 6,7-DMC in CTAB.

Results

Photoionization in Micelles. Radical cations of several psoralens and coumarins (Chart 1) were generated by photoionization in aqueous micellar solution, using the same approach that has been used in aqueous buffer.[9,10] Excitation of three psoralens (8-MOP, 5-MOP, and TMP) and three coumarins (7-MC, 5,7-DMC, and 6,7-DMC) at 355 nm in sodium dodecyl sulfate (SDS) resulted in the formation of the respective radical cations. Representative spectra of the radical cations in oxygen-saturated 0.1 M SDS are shown in Figure 1 for 5-MOP and 7-MC; the radical cations have λ_{max} at 550 and 630 nm. Spectra obtained for both 5-MOP and 7-MC show additional absorption at ∼500 nm at short time delays after the laser. This is due to the triplet excited state of the precursor, which is short-lived because of quenching by oxygen. Nitrogen-saturated solutions showed much larger triplet signals, in addition to broad absorptions due to the solvated electron, as described in previous work.[9,10] The results for 5-MOP are of particular interest because we had previously been unable to generate this radical cation by photoionization, although solubility problems had limited the experiments to aqueous acetonitrile, rather than buffer. The spectrum of the radical cation for each of the substrates was virtually identical to that obtained previously by either photoionization in aqueous buffer or aqueous acetonitrile or by

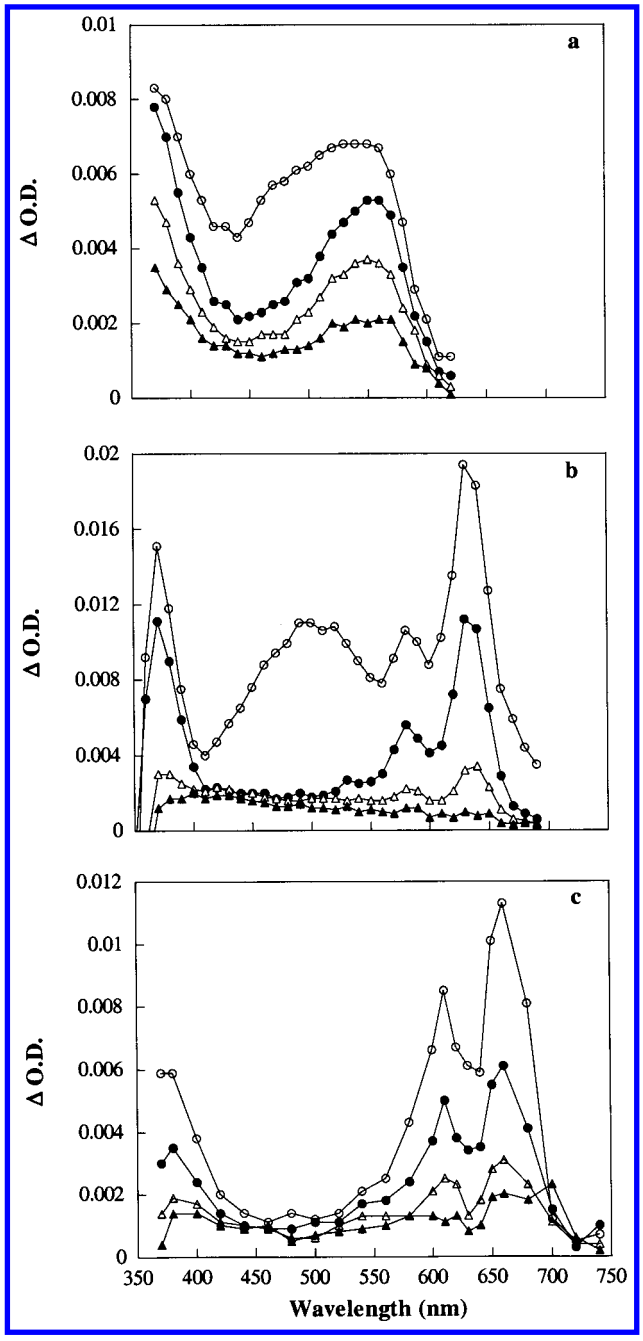

Figure 1. Transient absorption spectra obtained via 355 nm excitation of oxygen-saturated 0.1 M aqueous SDS solutions containing (a) 5-methoxypsoralen at delays of 0.7 μs (○), 1.7 μs (●), 6 μs (△), and 14 μs (▲) after the laser pulse, (b) 7-methoxycoumarin at delays of 5.6 μs (○), 17 μs (●), 82 μs (△), and 138 μs (▲) after the laser pulse, and (c) 4-aminomethyl-4,5′,8-trimethylpsoralen at delays of 3.2 μs (○), 7.6 μs (●), 14 μs (△), and 20 μs (▲) after the laser pulse.

photosensitized electron transfer using triplet chloranil in acetonitrile.[9,10]

One psoralen that had not been studied in earlier work was also photoionized in micellar solution. The spectrum of the radical cation obtained following 355 nm excitation of 4′-aminomethyl-4,5′,8-trimethylpsoralen (ATMP) in SDS solution has λ_{max} at 660 nm with a weaker band at 610 nm (Figure 1c) and is similar to that obtained from TMP. Small amounts of radical cation could be detected by photoionization in aqueous buffer, although the short lifetime of the radical cation (~0.3 μs) made it difficult to obtain spectra without contributions from both the solvated electron (700 nm) and the triplet (490 nm).

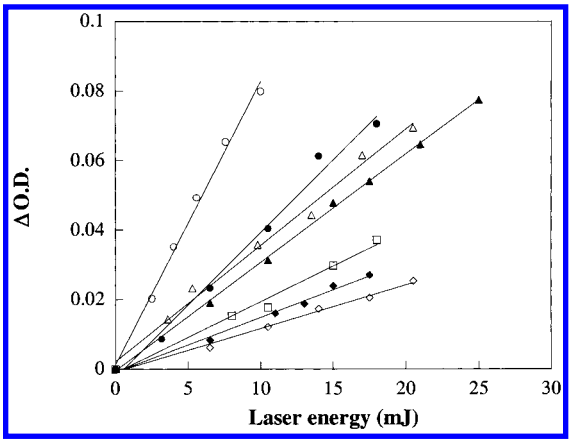

Figure 2. Plots of signal intensity for the solvated electron versus incident laser energy obtained via 355 nm excitation of nitrogen-saturated 0.1 M aqueous SDS solution containing 6,7-dimethoxycoumarin (●), 4,5′,8-trimethylpsoralen (△), 5,7-dimethoxycoumarin (▲), 7-methoxycoumarin (□), 8-methoxypsoralen (■), and 5-methoxypsoralen (◇). All solutions were matched with $\Delta OD_{355} = 0.4$ and benzophenone (○) in benzene was used as the actinometer.

TABLE 1: Quantum Yields of Photoionization (355 nm) of Psoralens and Coumarins in 0.1 M Aqueous SDS and Aqueous Phosphate Buffer[a]

	Φ_{pi} (0.1 M SDS)	Φ_{pi} (buffer)[b]
5-MOP	0.07	*c*
8-MOP	0.09	0.015
TMP[d]	0.19	0.02[e]
ATMP	0.16	*f*
7-MC	0.12	0.10
5,7-DMC	0.18	0.10
6,7-DMC[g]	0.24	0.20

[a] Errors are estimated as ±20%. [b] From ref 9. [c] Undetectable in 1:1 aqueous acetonitrile. [d] Quantum yields for TMP were 0.05 (0.03 M CTAB) and 0.08 (0.017 M Triton X-100). [e] In 1:1 aqueous acetonitrile. [f] Not determined. [g] Quantum yields for 6,7-DMC were 0.09 (0.03 M CTAB) and 0.12 (0.1 M Triton X-100).

The above results indicated that several of the psoralens were more readily ionized in aqueous micellar solution than in aqueous buffer. The radical cation yields for the various psoralens and coumarins were measured in 0.1 M SDS, using a similar approach to that employed previously for measurement of photoionization yields in aqueous solution.[9] The yields of solvated electron (700 nm) generated by excitation of the psoralen or coumarin and the yield of benzophenone triplet (525 nm) generated from an optically matched sample of benzophenone in benzene were measured as a function of laser energy. The plots of solvated electron yield vs laser energy (Figure 2) were linear for each of the compounds, consistent with monophotonic ionization as observed previously in aqueous solution.[9,10] In some cases, use of higher laser powers than those shown in Figure 2 gave plots with negative curvature, but no indication of the positive curvature associated with biphotonic behavior was detected. The measured quantum yields are listed in Table 1, along with data for most of the same substrates in aqueous solution. In each case, the photoionization efficiency in 0.1 M SDS is substantially higher than that in aqueous solution.

For comparison, the photoionization of 6,7-DMC and TMP was examined in both cationic and neutral micellar solution. The 355 nm excitation of both substrates in cetyltrimethylammonium bromide (CTAB) and Triton X-100 gave spectra that were identical to those obtained in SDS and in aqueous solution. Quantum yields for photoionization were also measured

TABLE 2: Fluorescence Maxima (±2 nm) for Selected Psoralens and Coumarins in Organic Solvents and Micellar Solution

	λ_{max}, nm		
solvent	6,7-DMC	7-MC	TMP
decane	386	377	384
cyclohexane	404		383
acetonitrile	420	378	422
buffer	431	388	468
0.1 M SDS	423	385	439
0.03 M CTAB	425	388	464
0.072 M Triton X-100	429	387	464

for CTAB and Triton X-100 (Table 1). In each case, the yields were considerably lower for the neutral Triton X-100 micelles as compared to those for either SDS or aqueous solution and yields were lower still in CTAB micelles.

Fluorescence of Psoralens and Coumarins. Fluorescence spectra of several of the substrates were measured in a number of different solvents and in micellar solution to provide evidence for the location of the substrate in the micelle. The data presented in Table 2 show that the fluorescence maximum shifts to significantly longer wavelength with increasing solvent polarity for each of the substrates. The largest shifts are observed for TMP for which λ_{max} shifts from 384 nm in decane to 468 nm in water. The fluorescence maxima for each of the substrates in SDS micelles indicate that the probe senses an environment with polarity intermediate between that of acetonitrile and that of water. For CTAB and Triton X-100 micelles, the fluorescence maxima are closer to those in water, indicating a slightly more polar environment than that for SDS. Note that similar data are available in the literature for these and related substrates in some of the same solvents, including micellar solutions;[29−32] the data in Table 2 provide a consistent set of data measured under the same conditions for correlation with the transient studies reported herein.

The change in fluorescence intensity as a function of surfactant concentration was used to estimate approximate partition coefficients (*K*, see Experimental Section for method) for two substrates for which most of the kinetic data were obtained. Values of ~8000 M^{-1} were estimated for 6,7-DMC and TMP in SDS solution and for 6,7-DMC in Triton X-100; a slightly larger value of 12 000 M^{-1} was estimated for 6,7-DMC in CTAB. These data can be used to provide estimates for the fraction of psoralen or coumarin associated with the micelles under our experimental conditions. For 0.1 M SDS, 92% of the substrate (either 6,7-DMC or TMP) will be localized in the micelle. The amounts of micelle-associated 6,7-DMC are 85% and 90% for 0.03 M CTAB and 0.05 M Triton X-100, respectively.[33]

Radical Cation Decay in the Absence and Presence of Quenchers. *a. Absence of Quenchers*. The kinetics for radical cation decay in SDS solution were significantly different from those in aqueous buffer. Good fits to a single exponential decay were obtained for oxygen-saturated samples for which any interference from either triplet excited precursor or the solvated electron appeared only as fast spikes on short time scales. As an example, the rate constant for decay of 6,7-DMC$^{\bullet+}$ was ~1 × 10^4 s^{-1} in 0.1 M SDS, approximately an order of magnitude less than that measured for the same radical cation in aqueous buffer at a similar precursor concentration (8 × 10^4 s^{-1}). The kinetics were slightly faster (~1.4 times) at lower surfactant concentration (0.017 M). The lifetime of the solvated electron measured at 710 nm (to avoid contributions from the radical cation) for oxygen-saturated SDS solutions is approximately 2 orders of magnitude shorter than that of the radical cation, with typical decay rate constants of ~(1−3) × 10^6 s^{-1}. The solvated electron decay varied from sample to sample, presumably due to variation in the oxygen concentration. Similar changes in radical cation kinetics were observed for TMP$^{\bullet+}$ for which typical decay rate constants were ~3 × 10^4 and ~1 × 10^5 s^{-1} in 0.1 M SDS and 20% acetonitrile/water, respectively. The decay of 6,7-DMC$^{\bullet+}$ was also slower in 0.03 M CTAB (2.5 × 10^4 s^{-1}) than in water, but the decay in Triton X-100 was similar to that in water. By contrast, the decay of TMP$^{\bullet+}$ was similar in both CTAB and Triton X-100 (1 × 10^6 s^{-1} and 8 × 10^5 s^{-1}) and was significantly faster than that in aqueous solution.

b. Anionic Quenchers. The decay of psoralen and coumarin radical cations is approximately an order of magnitude slower in SDS than in aqueous solution. This could result from localization of the radical cation at the micelle interface and subsequent protection from quenchers. However, given the relatively long lifetime of the radical cation, one must also consider the possibility that exit of the radical cation from the micelle and its subsequent decay in the aqueous phase are responsible for the observed kinetics. To distinguish between these two possibilities, we have used an approach similar to that used to estimate exit rates for triplet excited states from micelles.[28] This relies on the use of a quencher that is dissolved exclusively in the aqueous phase and is of opposite charge to the micellar interface. The model was originally developed with the assumption that quenching occurs only in the aqueous phase because of electrostatic repulsion between the quencher and the micelle interface. However, it has been extended to other supramolecular assemblies for which quenching of the complexed probe also occurs. This relies on the assumption that rate constants for quenching are significantly different for probes in aqueous solution and as part of a supramolecular complex.[23,34,35] Under these conditions, the rate constant for decay of the probe (k_{obs}) is given by eq 4; k_{mic} and k_0 are the decay of

$$k_{obs} = k_{mic} + k_- + k_{q,mic}[Q] - \frac{k_+ k_-[M]}{k_+[M] + k_0 + k_{q0}[Q]} \quad (4)$$

the probe in the micelle and in aqueous solution, k_{q0} and $k_{q,mic}$ are the rate constants for quenching of the probe in aqueous solution and in the micelle, and k_+ and k_- are entry and exit rate constants. Equation 4 predicts a nonlinear dependence of k_{obs} with increasing quencher concentration. If quenching of the micelle-incorporated probe is negligible, k_{obs} will level off to a limiting value of ($k_- + k_{mic}$). If quenching of the probe occurs with a substantially slower rate constant in the micelle phase, the plot at high quencher concentration will approach a linear relationship (eq 5), the slope of which gives $k_{q,mic}$. Note that

$$k_{obs} = k_{mic} + k_- + k_{q,mic}[Q] \quad (5)$$

the derivation of eq 4 relies on two additional requirements: the probe is localized predominantly in the micelle phase, and the probe decays with single-exponential kinetics.

To assess whether the radical cation exits from the micelle prior to reacting, the decay of 6,7-DMC$^{\bullet+}$ was measured in the presence of variable concentrations of two anionic quenchers, guanosine monophosphate (GMP) and nitrite ion. GMP has been shown to react with 6,7-DMC$^{\bullet+}$ in aqueous solution with a rate constant of 2.5 × 10^9 M^{-1} s^{-1}.[10] On the basis of its low oxidation potential (0.8 V vs SCE in water),[36] nitrite ion would also be expected to react efficiently. This was confirmed by measuring the decay of 6,7-DMC$^{\bullet+}$ in aqueous solution as a function of nitrite concentration, from which a rate constant of

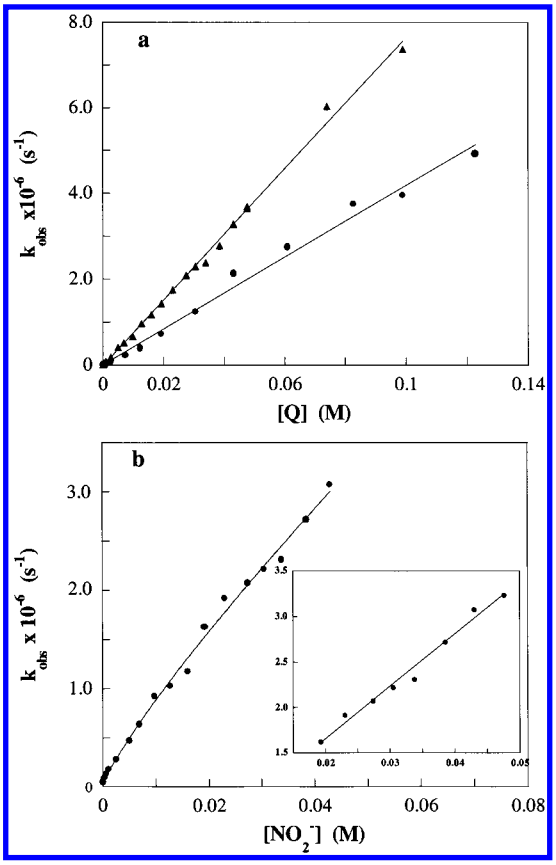

Figure 3. Dependence of the observed rate constants for decay of 6,7-DMC radical cation and triplet on quencher concentration in 0.1 M SDS. (a) Radical cation monitored at 590 nm. The solid lines correspond to the linear fitting of the data for nitrite (▲) and GMP (●). (b) Triplet monitored at 480 nm using nitrite as a quencher. The solid line corresponds to the fitting of the data to eq 4, with values for k_0, k_{q0}, and k_{mic} of 5.5×10^5 s^{-1}, 5.8×10^9 M^{-1} s^{-1}, and 4.2×10^4 s^{-1}, respectively. Inset: the solid line corresponds to linear fitting of the data at high nitrite concentrations (0.02−0.05 M).

1.7×10^9 M^{-1} s^{-1} was obtained. Nitrite quenching has been widely used to estimate exit rates for triplet probes from SDS micelles and thus has the advantage that it can be used to give estimates for exit of both triplet and radical cations from the micelle.

The decay of 6,7-DMC$^{\bullet+}$ was well-fit by single-exponential kinetics for all the quencher concentrations examined. Plots for radical cation decay in the presence of GMP and nitrite are shown in Figure 3a. Note that to measure the decay kinetics over a range of time scales, it is important to eliminate contributions due to the solvated electron, which absorbs over a broad range of visible wavelengths. For GMP quenching, this was accomplished by saturating the solutions with oxygen, which reduces the lifetime of both the triplet (measured at 480 nm) and the solvated electron (710 nm) without affecting the radical cation; the solubility of oxygen in aqueous SDS shortens the lifetime of the triplet and electron to <300 and 160 ns, respectively. Note that higher concentrations of GMP further decrease the solvated electron lifetime, although there is little effect on the triplet decay ($k_q < 10^8$ M^{-1} s^{-1}). N_2O-saturated solutions were used for the nitrite quenching experiments; this reduces the solvated electron lifetime to <20 ns, without affecting either triplet or radical cation so that the decay of both can be evaluated as a function of nitrite concentration.

The plots shown in Figure 3a indicate a linear dependence of k_{obs} with quencher concentration for both GMP and nitrite. The linearity over a wide range of time scales suggests that the exit of the radical cation is slow on the time scale of these experiments. The alternate possibility of rapid exit is inconsistent with the measured decay kinetics because the dependence of the radical cation decay on quencher concentration is very different from that in aqueous solution. The slope of the plots can thus be used directly as a measure of the rate constant for quenching of the micelle-incorporated radical cation. Values of 4.2×10^7 and 7.6×10^7 M^{-1} s^{-1} (Tables 3 and 4) were obtained for quenching of the micelle-incorporated 6,7-DMC$^{\bullet+}$ by GMP and nitrite, respectively. In each case, the quenching rate constant is almost 2 orders of magnitude less than that in aqueous solution.

TABLE 3: Estimates of Nitrite Quenching Rate Constants for Micelle-Incorporated Probes and Entry and Exit Rate Constants for the Probes in 0.1 M SDS and 0.056 M Triton X-100 Micelles[a]

probe	micelle	$k_{q,mic}$, 10^7 M^{-1} s^{-1}	k_-, 10^6 s^{-1}	k_+, 10^9 M^{-1} s^{-1}
6,7-DMC$^{\bullet+}$	SDS	7.6[b]		
^{3}DMC	SDS	5.6 ± 1.4	*d*	*d*
TMP$^{\bullet+}$[c]	SDS	5.1 ± 0.1	0.09 ± 0.02	2.1 ± 0.7
^{3}TMP[c]	SDS	5.4 ± 0.1	0.11 ± 0.03	3 ± 3
TMP$^{\bullet+}$	Triton X-100	40 ± 2	1.8 ± 0.2	1.0 ± 0.2
^{3}TMP	Triton X-100	40 ± 4	0.9 ± 0.4	7 ± 5

[a] The data are obtained by fitting data for nitrite quenching of TMP and 6,7-DMC triplets and radical cations to eq 4 using the parameters listed in the figure captions. The errors quoted are those obtained from fitting the data; in cases where multiple experiments were carried out, the data have all been used in the final fit. [b] Linear regression. [c] Data between 0 and 0.02 M (TMP$^{\bullet+}$) or 0−0.04 (^{3}TMP) used for fitting. [d] Errors obtained from the fit were in excess of 100%.

TABLE 4: Rate Constants for Reaction of Radical Cations with Selected Quenchers in 0.1 M SDS and in Aqueous Phosphate Buffer

		rate constants (M^{-1} s^{-1})		
probes	media	GMP	tryptophan	2,5-dimethyl-2,4-hexadiene
6,7-DMC	SDS	4.2×10^7	3.6×10^9	2.4×10^9
	buffer	2.5×10^9	3.0×10^9	2.6×10^{9b}
TMP	SDS	2.3×10^7	2.3×10^9	
	buffer	4.1×10^{9a}	6.9×10^{9a}	
8-MOP	SDS	3.2×10^7	2.7×10^9	5.2×10^9
	buffer	2.5×10^9	2.1×10^9	3.9×10^{9b}
7-MC	SDS	1.4×10^8	5.8×10^9	1.3×10^{10b}
	buffer	4.1×10^9	4.2×10^9	

[a] 1:1 aqueous acetonitrile. [b] Acetonitrile.

The decay of triplet 6,7-DMC at 480 nm was also measured as a function of nitrite concentration. In this case, the dependence of the triplet decay on quencher concentration is nonlinear with a curved region below ~0.015 M and linear behavior at higher concentrations (Figure 3b). The data were fit to eq 4, using our measured values of 5.5×10^5 and 4.2×10^4 s^{-1} for k_0 and k_{mic} and 5.8×10^9 M^{-1} s^{-1} for triplet quenching by nitrite in aqueous solution. The fit gives an estimate of 5.6×10^7 M^{-1} s^{-1} for $k_{q,mic}$. Linear fitting of the high-concentration data (>0.02 M) gives a similar result of 5.7×10^7 M^{-1} s^{-1} for $k_{q,mic}$ (inset, Figure 3b). Although fitting to eq 4 gives reasonably reliable estimates for $k_{q,mic}$, the errors for k_- and k_+ are large (>100%), so these parameters are not reported in Table 3.

A similar set of nitrite quenching experiments was carried out for TMP triplet and radical cation in aqueous SDS (Figure 4). The results for TMP$^{\bullet+}$ are analogous to those for 6,7-DMC$^{\bullet+}$ in that a linear dependence for radical cation decay on nitrite concentration is observed, the slope of which gives $k_{q,mic}$ of 6.0 $\times 10^7$ M^{-1} s^{-1}. However, close inspection of the data at low

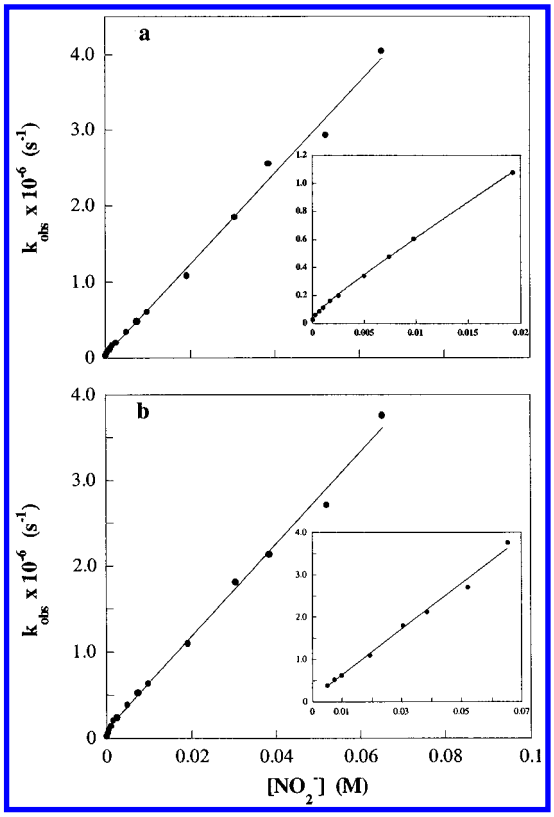

Figure 4. Dependence of the observed rate constants for decay of TMP radical cation and triplet on nitrite concentration in 0.1 M SDS. (a) Radical cation monitored at 640 nm. The solid line corresponds to the linear fitting of the data. Inset: the solid line corresponds to fitting of the data from 0 to 0.02 M nitrite to eq 4, with values for k_0, k_{q0}, and k_{mic} of 1.23×10^5 s^{-1}, 1.7×10^9 M^{-1} s^{-1}, and 2.9×10^4 s^{-1}, respectively. (b) Triplet monitored at 470 nm. The solid line corresponds to fitting of the data to eq 4, with values for k_0, k_{q0}, and k_{mic} of 1.85×10^5 s^{-1}, 5.8×10^9 M^{-1} s^{-1}, and 1.9×10^4 s^{-1}, respectively. Inset: the solid line corresponds to linear fitting of the data at high nitrite concentrations.

concentrations shows evidence for a curved region between 0 and 2.5 mM nitrite (inset in Figure 4a). Fitting the data to eq 4 gives a value of 5.1×10^7 M^{-1} s^{-1} for $k_{q,mic}$ and provides estimates of 8.6×10^4 s^{-1} and 2×10^9 M^{-1} s^{-1} for k_- and k_+. Although the errors are large, given the small range where nonlinearity is observed, it is clear that k_- is $<10^5$ s^{-1} for $TMP^{\bullet+}$. Because it is not possible to generate $TMP^{\bullet+}$ in aqueous solution, the fitting was done using the values for k_0 in 20% acetonitrile/water (1.2×10^5 s^{-1}) and k_{q0} measured for nitrite quenching of $DMC^{\bullet+}$ in water. A measured value of 2.9×10^4 s^{-1} for k_{mic} was used for fitting to eq 4.

For triplet TMP, plots of k_{obs} vs [NO_2^-] show curvature at low concentrations (Figure 4b). The fit to eq 4 (using the values for k_0, k_{mic}, and k_{q0} listed in the figure caption) and linear regression of the data in the high-concentration region (inset, Figure 4b) give an estimate of 5.4×10^7 M^{-1} s^{-1} for $k_{q,mic}$. Fitting to eq 4 gives values for k_- and k_+ of 1.1×10^5 s^{-1} and 3×10^9 M^{-1} s^{-1}, respectively. The error for k_+ is relatively large because the model is unable to recover accurate exit or entry rate constants when there is a large difference between the two.[23] In fact, simulations of the effect of varying k_- (using the values noted above for each of the other parameters) indicate that curvature at low concentrations is still clearly detectable at 10^5 s^{-1} but becomes negligible for slower exit rates.

Data for quenching of 8-MOP and 7-MC radical cations with GMP were also measured in 0.1 M SDS. These data have been obtained over a more limited concentration range, with the

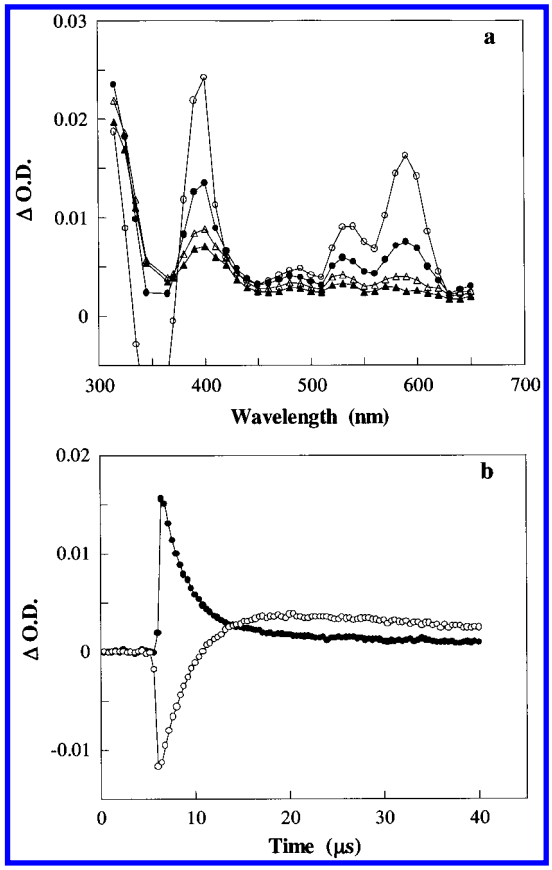

Figure 5. (a) Transient absorption spectra obtained via direct 355 nm excitation of 6,7-DMC in the presence of 5mM GMP in oxygen-saturated 0.1 M aqueous SDS solution at delays of 3.4 μs (○), 8.2 μs (●), 14 μs (△), and 20 μs (▲). (b) Decay kinetics monitored at 590 nm (●) and 365 nm (○).

assumption that the exit rate constants are $< 10^5$ s^{-1} in each case. Linear regression of the data gives the $k_{q,mic}$ values shown in Table 4. To confirm that the observed quenching occurs via electron transfer, as observed previously in aqueous solution,[8] transient spectra were measured for $6,7\text{-}DMC^{\bullet+}$ in the presence of 5 mM GMP. The spectra in Figure 5 show that the radical cation is observed at early time delays after the laser pulse, whereas at later delays, a weaker transient with a broad maximum at 390 nm is observed. Traces recorded at 365 nm (Figure 5) show a clear growth of the new species which is assigned to a GMP-derived radical formed by electron-transfer quenching of $6,7\text{-}DMC^{\bullet+}$. These results are in good agreement with our previous studies of reactions with mononucleotides in aqueous buffer and with literature reports for radicals derived from oxidation of GMP in aqueous solution at pH 7.[10,37,38]

The decay kinetics for TMP triplet and radical cation were also measured in Triton X-100 as a function of nitrite concentration. The data obtained are shown in Figure 6. The data for the radical cation show a clear break at ~1 mM nitrite, with a linear region at higher concentrations (Figure 6a). The data obtained for $k_{q,mic}$, k_-, and k_+ are listed in Table 3. Note that the entry and exit rate constants are much better defined for TMP in Triton X-100 than for any of the data in SDS. Because the exit rate constant is now approximately an order of magnitude faster, no attempts were made to measure the reactivity of other radical cations with anionic quenchers in Triton X-100. The TMP triplet data (Figure 6b) show both curved (below ~2 mM) and linear regions. The parameters extracted from the fit are also given in Table 3. In this case, the large difference between k_- and k_+ again leads to substantial

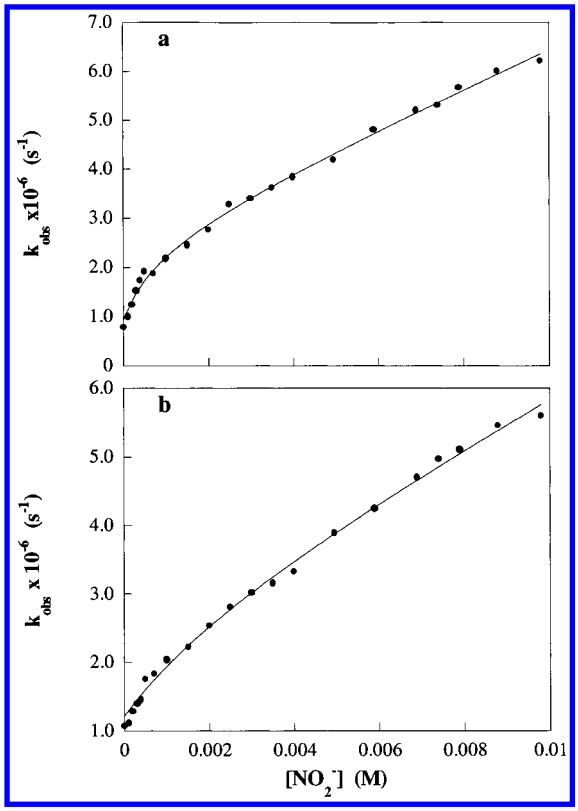

Figure 6. Dependence of the observed rate constants for decay of TMP radical cation and triplet on nitrite concentration in 0.056 M Triton X-100. (a) Radical cation monitored at 640 nm. The solid line corresponds to the fitting of the data to eq 4, with values for k_0, k_{q0}, and k_{mic} of 1.23×10^5 s^{-1}, 1.7×10^9 M^{-1} s^{-1}, and 7.8×10^5 s^{-1}, respectively. (b) Triplet monitored at 470 nm. The solid line corresponds to the fitting of the data to eq 4, with values for k_0, k_{q0}, and k_{mic} of 1.85×10^5 s^{-1}, 5.8×10^9 M^{-1} s^{-1}, and 1.2×10^6 s^{-1}, respectively.

uncertainty in the recovery of these parameters, as reflected by the reported errors in Table 3.

c. Neutral and Zwitterionic Quenchers. The decay of 6,7-DMC$^{\bullet+}$ in SDS was measured in the presence of tryptophan and 2,5-dimethyl-2,4-hexadiene. The decay traces gave good fits to single-exponential kinetics, and plots of radical cation decay as a function of quencher concentration were linear over the range of concentrations studied. On the basis of the results with anionic quenchers, the decay of the observed radical cations occurs exclusively in the micelle. This might be expected to lead to multiexponential kinetics for quenchers that are solubilized in the micelle, as a result of a distribution of quencher occupancies/micelle for any given concentration. The single-exponential decay indicates that exchange of quenchers between the aqueous and micellar phases is rapid on the time scale of the radical cation decay. In such cases, the data can be treated using a pseudophase model that considers the micellar solution as a two-phase system, composed of a bulk aqueous phase and a micellar pseudophase.[6,39] The quenching rate constant can be obtained via eq 6 where the concentration used ($[Q]_{mic}$) is that in the micelle phase and k_{mic} corresponds to the rate constant for probe decay in the micelle phase.

$$k_{obs} = k_{mic} + k_{q,mic}[Q]_{mic} \qquad (6)$$

If the above assumptions are valid, the slope of the plots of radical cation decay vs quencher concentration provide a direct measure of the quenching rate constants, after correction for the fraction of quencher in the micellar phase. Literature values of 7×10^6 and 5×10^9 s^{-1} have been reported [40] for k_- and k_+ for the tryptophan zwitterion, the main species present at pH 7. This confirms that at least for tryptophan the exchange of quencher is rapid on the time scale of radical cation decay, as long as k_{obs} is less than approximately 3×10^6 s^{-1}. The reported partition coefficient of 690 M^{-1} for the tryptophan zwitterion can be used to estimate that 52% of the total tryptophan is incorporated in the micelle. After correction, a quenching rate constant of 3.6×10^9 M^{-1} s^{-1} is obtained for reaction of 6,7-DMC$^{\bullet+}$ with tryptophan. Similar analysis gives the rate constants shown in Table 4 for several other radical cations. Evidence for electron-transfer quenching of psoralen and coumarin radical cations by tryptophan was also provided by the detection of the radical formed by deprotonation of the initially formed tryptophan radical cation.

Similarly, the reported partition coefficient of 2500 M^{-1} for 2,5-dimethyl-2,4-hexadiene indicates that 75% of the diene is incorporated in the micelle for 0.1 M SDS.[41] This and the slope of plots of k_{obs} vs diene concentration were used to calculate the rate constants shown in Table 4. Although entry and exit rate constants do not appear to be available for this particular diene, making the reasonable assumption of $k_+ \approx 5 \times 10^9$ M^{-1} s^{-1} gives an estimate of $\sim 2 \times 10^6$ s^{-1} for k_-. We have also observed linear plots for reaction of both histidine and 8,10-dodecadienol with psoralen and coumarin radical cations, but partition coefficients are not available for these quenchers.

Discussion

Radical cations of a variety of psoralens and coumarins can be generated efficiently by photoionization in aqueous SDS; the spectra of the radical cations are virtually identical to those obtained in aqueous solution. This is consistent with fluorescence results indicating that the psoralen and coumarin substrates examined are localized near the micellar interface in a relatively polar environment. The transient experiments have been carried out at high surfactant concentrations to ensure that >90% of the substrate is localized in the micelle, thus minimizing the possibility of excitation of residual substrate in the aqueous phase. The quantum yield for radical cation formation for each substrate is significantly higher in SDS than in aqueous buffer or aqueous acetonitrile. Initial photoionization of the micelle-associated substrate will generate an electron that is rapidly repelled from the negatively charged micellar interface into the aqueous phase; conversely, electrostatic effects will favor association of the radical cation with the micelle. This rapid separation of the initial electron/radical cation pair leads to an enhanced photoionization yield despite the fact that the overall polarity sensed by the substrate is somewhat lower than that in aqueous solution. Enhanced photoionization yields in anionic micelles have been reported for a variety of aromatic hydrocarbons and amines and even an aromatic ketone.[2,42−44] By contrast to the results for psoralens and coumarins, in most previously reported examples, the photoionization process is biphotonic, although one-photon ionization has been observed for several aromatic amines that are localized close to the micelle surface rather than in the hydrocarbon core.[42] The present work provides an additional example of the control of charge separation via electrostatic effects and also permits a direct comparison of the photoionization yields in homogeneous and micellar solution.

For two substrates, we have also compared the photoionization yields in cationic and neutral micelles with those in aqueous buffer and SDS micelles. For both 6,7-DMC and TMP, the yields in Triton X-100 and CTAB micelles are approximately 2−3 times lower than those in SDS; for 6,7-DMC, the yields

are also significantly lower than those in aqueous buffer. The lower quantum yields in neutral micelles are consistent with a decreased photoionization efficiency due to the less polar environment of the micellar interface as compared to aqueous solution and are similar to our previous observations of lower yields in aqueous acetonitrile.[9]

The photoionization yields are lowest in CTAB for which there is no driving force for efficient separation of the electron from the positively charged micellar interface. Although electrostatic repulsion of the relatively large radical cation may favor its eventual redistribution to the aqueous phase, this is unlikely to occur sufficiently rapidly to compete with back electron transfer in the initial geminate radical cation/electron pair. Thus, both the positively charged interface and the restricted environment of the micelle contribute to an enhanced recombination of the initial electron/radical cation pair and a lower photoionization yield. Note that the lower yield is despite the fact that the fluorescence data indicate that the substrate is located in a more polar environment in both Triton X-100 and CTAB than in SDS. Although the radical cation does not exit to the aqueous phase sufficiently rapidly to compete with geminate recombination, it is likely that exit occurs much more rapidly than decay of the radical cation within the micelle.

Quenching of 6,7-DMC$^{\bullet+}$ and TMP$^{\bullet+}$ in SDS with anionic nucleophiles that are expected to remain in the aqueous phase gives linear plots over a wide range of quencher concentrations consistent with slow exit of the radical cation from the micellar phase. For both 6,7-DMC$^{\bullet+}$ and TMP$^{\bullet+}$, we estimate that $k_- < 10^5$ s^{-1}. This can be contrasted with the behavior of TMP$^{\bullet+}$ in Triton X-100, for which curved quenching plots are obtained, allowing an estimate of 1.8×10^6 s^{-1} for k_-. This indicates that electrostatic effects are important in determining the residence time of the radical cation in the micellar phase, with at least an order of magnitude enhancement in the rate at which the radical cation exits the neutral micelle. Electrostatics also play a role in the determining the affinity of the radical cation for the micelle because k_+ for TMP$^{\bullet+}$ in Triton X-100 is approximately half that in SDS. The measured exit and entry rate constants can be used to calculate K_{eq} of 550 M^{-1} for TMP$^{\bullet+}$ in Triton X-100 as compared to 23 000 M^{-1} in SDS.

The results for nitrite quenching allow a direct comparison of the behavior of the TMP triplet and radical cations. The measured entry and exit rate constants give K_{eq} values of 7800 and 33 000 M^{-1} for triplet TMP in Triton X-100 and SDS. By contrast to the results for the radical cation for which K is approximately 42 times larger in SDS than in Triton X-100, the equilibrium constant for triplet TMP is only 4 times higher in SDS than in Triton X-100. Thus, electrostatic stabilization of the charged radical ion leads to a factor of 10 enhancement in the affinity of the radical cation for the micelle, as compared to the triplet excited state of the same probe. The equilibrium constants for triplet TMP are of similar magnitude to those measured for a variety of triplet ketones in SDS micelles.[45−47] This is consistent with the fact that both the ketones and the psoralens and coumarins studied herein are solubilized in the relatively polar micellar interface region. This can be contrasted with the higher equilibrium constants (typically 10^5-10^6 M^{-1}) measured for less polar aromatic hydrocarbons. Although we have not been able to find any data for exit of radical cations from micelles, styrene radical cations have recently been shown to escape from neutral cyclodextrin cavities in less than 100 ns.[48]

The quenching results clearly demonstrate that the micelle-solubilized triplets and radical cations are accessible to anionic quenchers, both in Triton X-100 and in SDS. For SDS, the quenching rate constants are approximately 2 orders of magnitude lower than those in aqueous solution for both triplets and radical cations. In Triton X-100, the difference in quenching rate constants is roughly 1 order of magnitude, consistent with the increased accessibility of the quencher for the neutral micelle in the absence of electrostatic repulsion. Note that these results may be contrasted with literature data for some aromatic hydrocarbons for which the rate constants for quenching of the micelle-incorporated triplet have been assumed to be negligible.[28] However, in this case, the probe is expected to be solubilized in the hydrocarbon core of the micelle and thus much better protected from aqueous-phase quenchers than are the psoralens and coumarins studied in the present work. The present results are analogous to those for probes complexed to cyclodextrins and bile salt aggregates where quenching of both complexed and uncomplexed probes occurs, although with significantly different rate constants.[35]

The slow exit rate constants for radical cations in SDS make it straightforward to measure quenching rate constants for both anionic and neutral quenchers for a number of radical cations. The rate constants for GMP are between 1 and 2 orders of magnitude lower than those in aqueous solution, further demonstrating the effect of electrostatic repulsion in modulating the reactivity of the micelle-incorporated radical cation. Nevertheless, the rate constant for 7-MC is approximately three times larger than that for 6,7-DMC, indicating that the oxidation potential of the substrate (and hence the driving force for electron transfer) still plays an important role in determining the overall reactivity.

Rate constants for electron-transfer quenching by neutral and zwitterionic quenchers are similar in water and anionic micelles; if anything, the estimated k_q values are slightly faster in SDS than in water. However, it is worth noting that electron transfer for the two substrates that we have examined is exoergonic by >0.2 eV.[9,49,50] Effects of micelle incorporation are more likely to be detected for reactions that are less exoergonic and occur with rates that are significantly below the diffusion-controlled limit. The minimal effect is in line with literature data for electron-transfer reactions between excited SDS-bound ruthenium tris(2,2′-bipyridyl) and a series of micelle-solubilized quenchers for which the rate constants and energetics are similar to those in aqueous solution.[6] By contrast, electron-transfer quenching of the excited state of an aqueous ruthenium complex by diheptyl viologen bound to SDS micelles is over an order of magnitude slower than the same reaction in aqueous solution.[7] The present results indicate that radical cations provide excellent probes for studying electron-transfer reactivity in anionic micelles. Their utility could be further enhanced by using a psoralen with a larger alkyl substituent in place of methyl to further reduce the rate at which the radical cation exits from the micelle.

The results described above for the generation and reactivity of psoralen and coumarin radical cations demonstrate that it is crucial to understand the effect of the microenvironment on partitioning of excited states and reactive intermediates between various reaction pathways. For example, both polarity and electrostatic effects are important in determining the yield of the initial photoionization step and in controlling the fate of the radical cations that are generated. Any detailed understanding of the in vivo photochemistry of psoralen drugs will have to take into account the site of localization and how this may control the overall chemistry. Although in many ways a micelle is a very crude approximation for the cellular environment, it

has proven useful in delineating the importance of electrostatic effects, polarity, and mobility in affecting the dynamics of radical cations. These factors will be equally important (although perhaps harder to quantify) for understanding the behavior of psoralens in vesicles or as DNA or protein complexes. Such studies are in progress.

References and Notes

(1) Gratzel, M. In *Solar Energy Harvesting*; Gratzel, M., Ed.; Elsevier: New York, 1988; pp 394−440.

(2) Kalyanasundaram, K. *Photochemistry in Microheterogeneous Systems*; Academic Press: Orlando, FL, 1987.

(3) Fox, M. A. *Top. Curr. Chem.* **1991**, *159*, 67−101.

(4) Turro, N. J. *Pure Appl. Chem.* **1995**, *67*, 199−208.

(5) Weidemaier, K.; Tavernier, H. L.; Fayer, M. D. *J. Phys. Chem. B* **1997**, *101*, 9352−9361.

(6) Soboleva, I. V.; van Stam, J.; Dutt, G. B.; Kuzmin, M. G.; De Schryver, F. C. *Langmuir* **1999**, *15*, 6201−6207.

(7) Hackett, J. W., II; Turro, C. *J. Phys. Chem. A* **1998**, *102*, 5728−5733.

(8) Wood, P. D.; Mnyusiwalla, A.; Chen, L.; Johnston, L. J. *Photochem. Photobiol.* **2000**, *72*, 155−162.

(9) Wood, P. D.; Johnston, L. J. *J. Phys. Chem.* **1998**, *102*, 5585−5591.

(10) Wood, P. D.; Johnston, L. J. *Photochem. Photobiol.* **1997**, *66*, 642−648.

(11) Gasparro, F. P. *Psoralen DNA Photobiology*; CRC Press: Boca Raton, FL, 1988; Vols. 1 and 2.

(12) Pathak, M. A.; Fitzpatrick, T. B. *J. Photochem. Photobiol., B: Biol.* **1992**, *14*, 3−22.

(13) Bensasson, R. V.; Land, E. J.; Truscott, T. G. *Excited States and Free Radicals in Biology and Medicine*; Oxford University Press: Oxford, 1993.

(14) Goodrich, R. P.; Yerram, N. R.; Tay-Goodrich, B. H.; Forster, P.; Platz, M. S.; Kasturi, C.; Park, S. C.; Aebischer, J. N.; Rai, S.; Kulaga, L. *Proc. Natl. Acad. Sci. U.S.A.* **1994**, *91*, 5552−5556.

(15) Gonzalez, E. *Dermatol. Clin.* **1995**, *13*, 851−866.

(16) Stern, R. S.; Nichols, K. T.; Vakeva, L. H. *N. Engl. J. Med.* **1997**, *336*, 1041−1045.

(17) Young, A. R. *J. Photochem. Photobiol., B: Biol.* **1990**, *6*, 237−247.

(18) Blan, Q. A.; Grossweiner, L. I. *Photochem. Photobiol.* **1987**, *45*, 177−183.

(19) Bordin, F.; Conconi, M. T.; Capozzi, A. *Photochem. Photobiol.* **1987**, *46*, 301−304.

(20) Dall'Acqua, F.; Martelli, P. *J. Photochem. Photobiol., B: Biol.* **1991**, *8*, 235−254.

(21) Sastry, S. S.; Ross, B. M.; P'arraga, P. *J. Biol. Chem.* **1997**, *272*, 3715−3723.

(22) Schmitt, I. M.; Chimenti, S.; Gasparro, F. P. *J. Photochem. Photobiol., B: Biol.* **1995**, *27*, 101−107.

(23) Kleinman, M. H.; Bohne, C. *Org. Photochem.* **1997**, *1*, 391−466.

(24) Kazanis, S.; Azarani, A.; Johnston, L. J. *J. Phys. Chem.* **1991**, *95*, 4430−4435.

(25) Carmichael, I.; Helman, W. P.; Hug, G. L. *J. Phys. Chem. Ref. Data* **1987**, *6*, 239.

(26) Fielden, E. M.; Hart, E. J. *Radiat. Res.* **1967**, *32*, 564−580.

(27) Bohne, C.; Redmond, R. W.; Scaiano, J. C. In *Photochemistry in Organized and Constrained Media*; Ramamurthy, V., Ed.; VCH Publishers Inc.: New York, 1991; Chapter 3.

(28) Almgren, M.; Grieser, F.; Thomas, J. K. *J. Am. Chem. Soc.* **1979**, *101*, 279−291.

(29) Becker, R.; Chakravorti, S.; Gartner, C. A.; de Graca Miguel, M. *J. Chem. Soc., Faraday Trans.* **1993**, *89*, 1007−1019.

(30) Muthuramu, K.; Ramamurthy, V. *J. Photochem.* **1984**, *26*, 57−64.

(31) Paik, Y. H.; Shim, S. C. *J. Photochem. Photobiol., A: Chem.* **1991**, *56*, 349−358.

(32) Sousa, C.; Sa e Melo, T. *Photochem. Photobiol.* **1996**, *63*, 182−186.

(33) CMC values used to calculate the micelle concentrations are 8.1 mM, 9.0 mM, and 0.9 mM for SDS, Triton X-100, and CTAB, and aggregation numbers are 70, 35, and 61, respectively. Fendler, J. H.; Fendler, E. J. *Catalysis in Micellar and Macromolecular Systems*; Academic Press: New York, 1975.

(34) Turro, N. J.; Okubo, T.; Chung, C.-J. *J. Am. Chem. Soc.* **1982**, *104*, 1789−1794.

(35) Ju, C.; Bohne, C. *J. Phys. Chem.* **1996**, *100*, 3847−3854.

(36) Wayner, D. D. M. In *Handbook of Organic Photochemistry*; Scaiano, J. C., Ed.; CRC Press: Boca Raton, FL, 1989; Vol. II, Chapter 18.

(37) Faraggi, M.; Broitman, F.; Trent, J. B.; Klapper, M. H. *J. Phys. Chem.* **1996**, *100*, 14751−14761.

(38) Gut, I. G.; Wood, P. D.; Redmond, R. W. *J. Am. Chem. Soc.* **1996**, *118*, 2366−2373.

(39) Bunton, C. A.; Nome, F.; Quina, F. H.; Romsted, L. S. *Acc. Chem. Res.* **1991**, *24*, 357−364.

(40) Encinas, M. V.; Lissi, E. A. *Photochem. Photobiol.* **1986**, *44*, 579−585.

(41) Encinas, M. V. *J. Phys. Chem.* **1983**, *87*, 4770−4772.

(42) Thomas, J. K.; Piciulo, P. L. *J. Am. Chem. Soc.* **1978**, *101*, 2502−2503.

(43) Hashimoto, S.; Thomas, J. K. *J. Photochem. Photobiol., A: Chem.* **1991**, *55*, 377−386.

(44) Boch, R.; Whittlesey, M. K.; Scaiano, J. C. *J. Phys. Chem.* **1994**, *98*, 7854−7857.

(45) Martinez, L. J.; Scaiano, J. C. *J. Phys. Chem. A* **1999**, *103*, 203−208.

(46) Mohtat, N.; Cozens, F. L.; Scaiano, J. C. *J. Phys. Chem. B* **1998**, *102*, 7557−7562.

(47) Scaiano, J. C.; Selwyn, J. C. *Can. J. Chem.* **1981**, *59*, 2368−2372.

(48) Murphy, R. S.; Bohne, C. *Photochem. Photobiol.* **2000**, *71*, 35−43.

(49) Jovanovic, S. V.; Steenken, S. *J. Phys. Chem.* **1992**, *96*, 6674−6679.

(50) Schepp, N. P.; Johnston, L. J. *J. Am. Chem. Soc.* **1994**, *116*, 10330−10331.